

Missing Data Imputation and Acquisition with Deep Hierarchical Models and Hamiltonian Monte Carlo

Ignacio Peis^{1*}, Chao Ma^{2,3}, José Miguel Hernández-Lobato²

¹Universidad Carlos III de Madrid, Spain

²University of Cambridge, UK

³Microsoft Research Cambridge, UK

Universidad
Carlos III
de Madrid



UNIVERSITY OF
CAMBRIDGE

NEURAL INFORMATION
PROCESSING SYSTEMS
New Orleans, USA, 2022

Summary

- **Goal: impute, predict, acquire information** from heterogeneous incomplete data using $p(x_i, \mathbf{y} | \mathbf{x}_O) \approx \mathbb{E}_{q^{(T)}(\mathbf{h} | \mathbf{x}_O)} [p(x_i, \mathbf{y} | \mathbf{h})]$, where samples from $q^{(T)}(\mathbf{h} | \mathbf{x}_O)$ approximately follow the true posterior.
- We present **HH-VAEM**, a **deep hierarchical model** for handling mixed-type incomplete data with **automatically tuned HMC**.
- We propose a **sampling-based strategy for feature acquisition** that benefits from the improved inference of HH-VAEM.

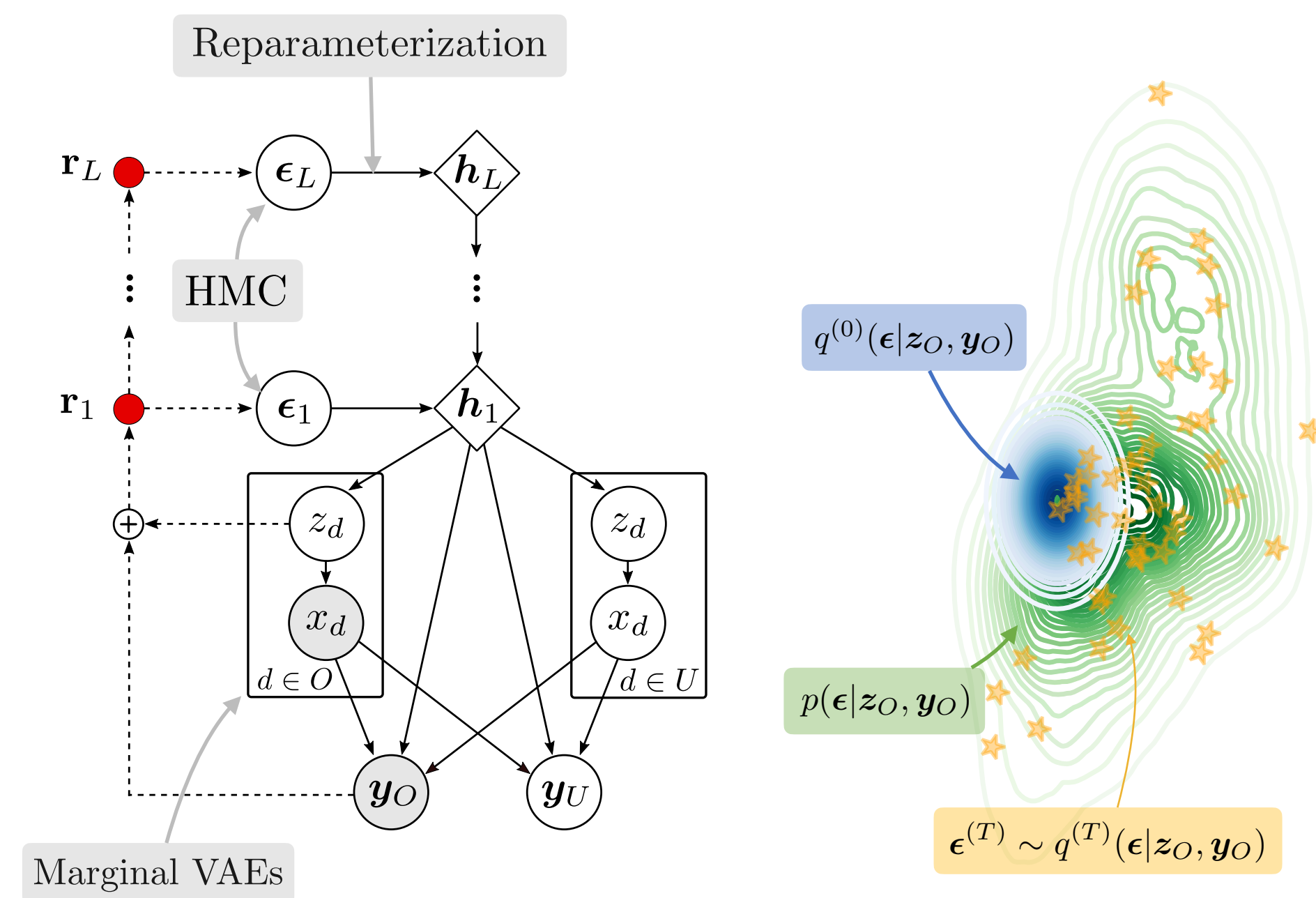


Figure 1: HH-VAEM model (left) and HMC example (right).

Hierarchical VAE and HMC

- Increase model flexibility with a **hierarchical latent space** $\mathbf{h} = \{h_1, \dots, h_L\}$ where $h_l \sim p(h_l | h_{l+1})$.
- **Reparameterization** for reducing strong curvature regions where $\nabla_{\mathbf{h}_{1:L}} \log p^*(\mathbf{h}_{1:L}) \uparrow \uparrow$:
$$h_l = f_{\mu_l}(h_{l+1}) + f_{\sigma_l}(h_{l+1}) \cdot \epsilon_l$$
- Improving posterior approximation by means of **well-posed HMC** to sample $\epsilon^{(T)} \sim q^{(T)}(\epsilon | z_O, \mathbf{y}_O)$.
- **Automatically tune HMC hyperparams** for efficiently explore posterior distribution.

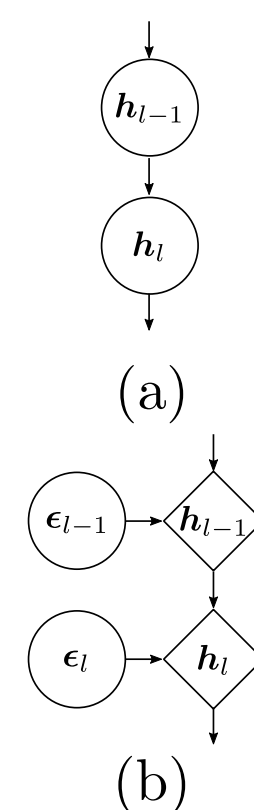


Figure 2: AR (a), Reparam. (b).

Motivation

Low bias samples from HMC and hierarchically enriched model improve the three considered tasks:

- **Imputation:** $p(\mathbf{x}_U | \mathbf{x}_O) \approx \mathbb{E}_{q^{(T)}(\epsilon | \mathbf{x}_O)} [p(\mathbf{x}_U | \epsilon)]$.
- **Prediction:** $p(\mathbf{y} | \mathbf{x}_O) \approx \mathbb{E}_{q^{(T)}(\epsilon | \mathbf{x}_O)} [p(\mathbf{y} | \epsilon, \mathbf{x}_O, \hat{\mathbf{x}}_U)]$.
- **Sampling-based active learning.**

Training

1. Train **marginal VAEs** $\{\theta_d, \gamma_d\}_{d=1}^D$ to standardize heterogeneous data.
2. **Pre-train dependency VAE** $\{\psi, \theta_z, \theta_y\}$ using \mathcal{L}_{VI} .
3. **Fine-tune** encoder using \mathcal{L}_{VI} , decoder, predictor and **HMC hyperparams** ϕ using \mathcal{L}_{HMC} with initial proposal $q^{(0)}$ inflated by s , and **inflation parameter** s using \mathcal{L}_{SKSD} .

$$\mathcal{L}_{VI}(z_O, \mathbf{y}_O; \{\theta, \psi\}) = \mathbb{E}_{q_\psi} \left[\log \frac{p_\theta(z_O, \mathbf{y}_O, \epsilon)}{q_\psi(\epsilon | z_O, \mathbf{y}_O)} \right]$$

$$\mathcal{L}_{HMC}(z_O, \mathbf{y}_O; \{\theta, \phi\}) = \mathbb{E}_{q_\phi^{(T)}(\epsilon)} [\log p_\theta(z_O, \mathbf{y}_O, \epsilon)]$$

$$\mathcal{L}_{SKSD}(z_O, \mathbf{y}_O; \mathbf{s}) = \text{SKSD} \left(q_\phi^{(T)}(\epsilon | z_O, \mathbf{y}_O; \mathbf{s}), p(\epsilon | z_O, \mathbf{y}_O) \right)$$

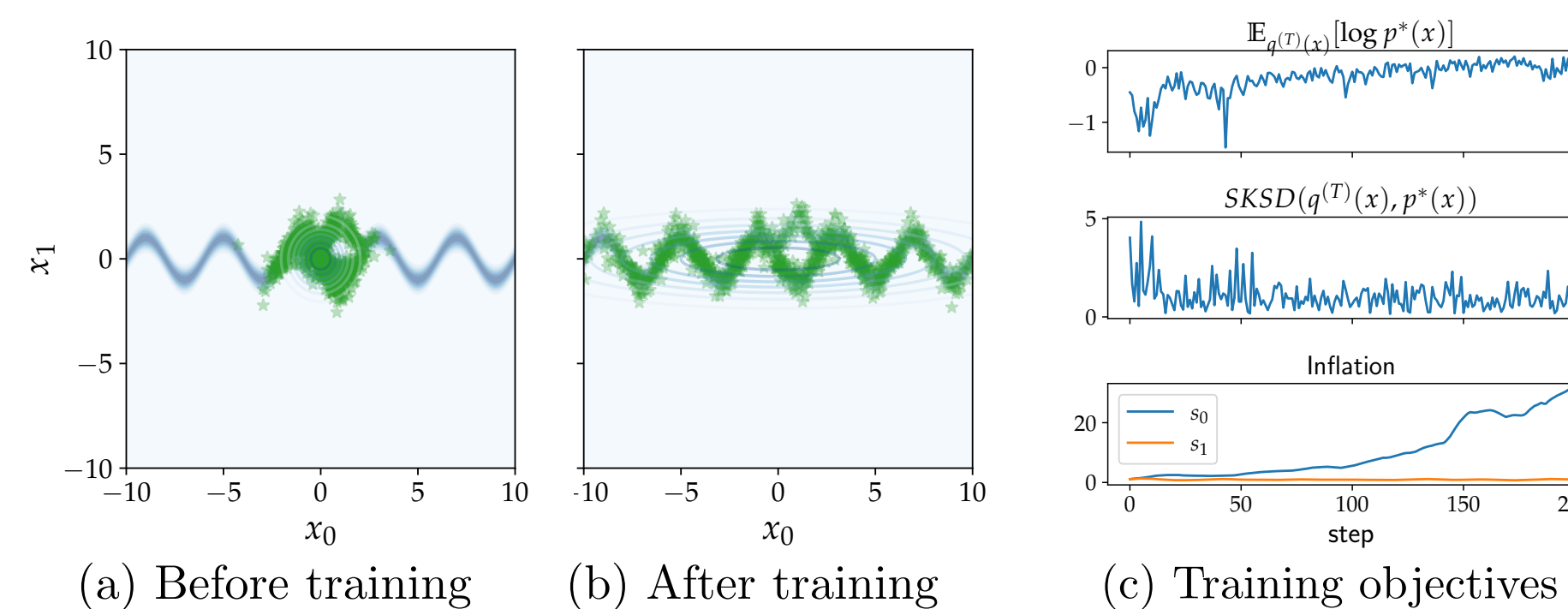


Figure 3: HMC training example.

Sampling-Based Active Learning

- **Sampling-based** information reward estimator for acquiring variables x_i to accurately predict \mathbf{y} :

$$\hat{R}_I = \hat{I}(\mathbf{y}, x_i | \mathbf{x}_O) \approx \sum_{ij} \hat{p}_{x_i, \mathbf{y} | \mathbf{x}_O}(i, j) \log \frac{\hat{p}_{x_i, \mathbf{y} | \mathbf{x}_O}(i, j)}{\hat{p}_{x_i | \mathbf{x}_O}(i) \hat{p}_{\mathbf{y} | \mathbf{x}_O}(j)}$$

that uses **HMC** in $p(x_i, \mathbf{y} | \mathbf{x}_O) \approx \mathbb{E}_{q^{(T)}(\epsilon | \mathbf{x}_O)} [p(x_i, \mathbf{y} | \epsilon)]$, instead of the **Gaussian** alternative (Figure 1).

Experiments

		VAE(M)	MIWAE(M)	H-VAE(M)	HMC-VAE(M)	HH-VAE(M)
$-\log p(\mathbf{x}_U \mathbf{x}_O)$	MNIST	0.124 ± 0.001	0.121 ± 0.001	0.119 ± 0.001	0.101 ± 0.004	0.094 ± 0.00
	F-MNIST	0.162 ± 0.002	0.160 ± 0.002	0.156 ± 0.002	0.150 ± 0.002	0.144 ± 0.00
	Avocado	1.89 ± 0.01	1.92 ± 0.04	1.89 ± 0.01	1.89 ± 0.02	1.88 ± 0.0
$-\log p(\mathbf{y} \mathbf{x}_O)$	Bank	2.84 ± 0.07	2.74 ± 0.05	2.82 ± 0.06	2.69 ± 0.05	2.63 ± 0.0
	MNIST	0.153 ± 0.009	0.151 ± 0.007	0.146 ± 0.006	0.067 ± 0.007	0.056 ± 0.01
	F-MNIST	0.501 ± 0.012	0.496 ± 0.008	0.494 ± 0.007	0.357 ± 0.060	0.337 ± 0.06
Accuracy	Avocado	1.18 ± 0.02	1.15 ± 0.03	1.18 ± 0.02	1.12 ± 0.03	1.10 ± 0.0
	Bank	0.56 ± 0.06	0.51 ± 0.03	0.50 ± 0.03	0.52 ± 0.02	0.49 ± 0.0
Accuracy	MNIST	0.953 ± 0.004	0.953 ± 0.003	0.953 ± 0.003	0.978 ± 0.003	0.981 ± 0.00
	F-MNIST	0.824 ± 0.005	0.824 ± 0.004	0.824 ± 0.004	0.869 ± 0.015	0.876 ± 0.01

Table 1: Imputation and prediction evaluation.

$$\log p(\mathbf{x}_U | \mathbf{x}_O) \approx \log \mathbb{E}_{q^{(T)}(\epsilon | \mathbf{x}_O)} [p(\mathbf{x}_U | \epsilon)] \approx \log \frac{1}{k} \sum_i p(\mathbf{x}_U | \epsilon_i^{(T)})$$

$$\log p(\mathbf{y} | \mathbf{x}_O) \approx \log \mathbb{E}_{q^{(T)}(\epsilon | \mathbf{x}_O)} [p(\mathbf{y} | \epsilon, \hat{\mathbf{x}})] \approx \log \frac{1}{k} \sum_i p(\mathbf{y} | \epsilon_i^{(T)}, \hat{\mathbf{x}}_i)$$

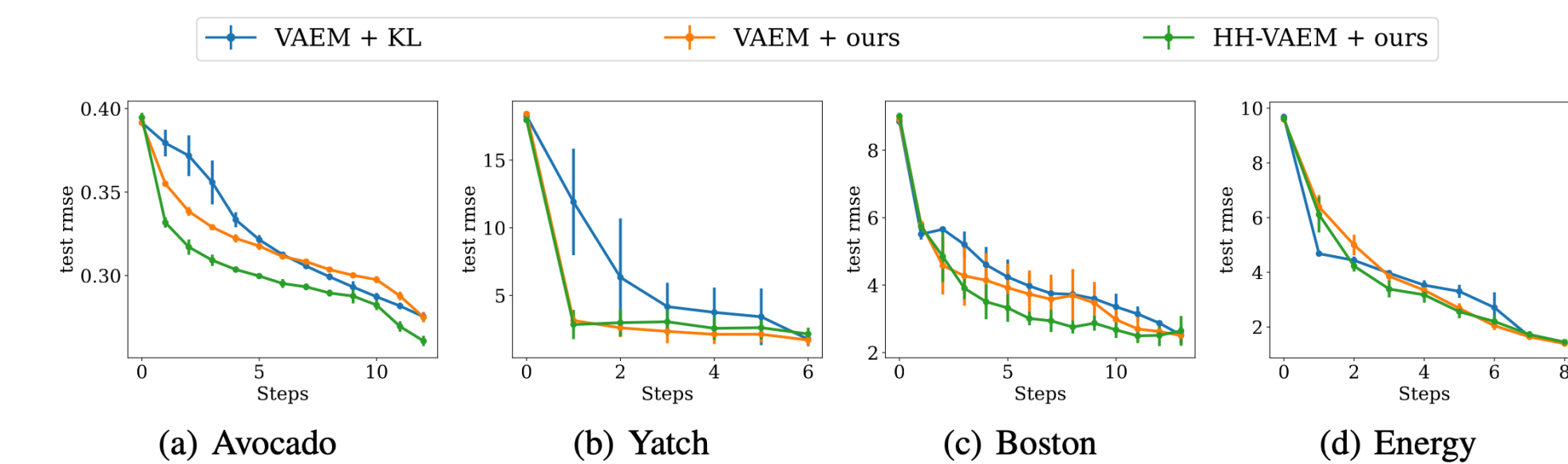


Figure 4: SAIA curves. RMSE vs number of discovered features.

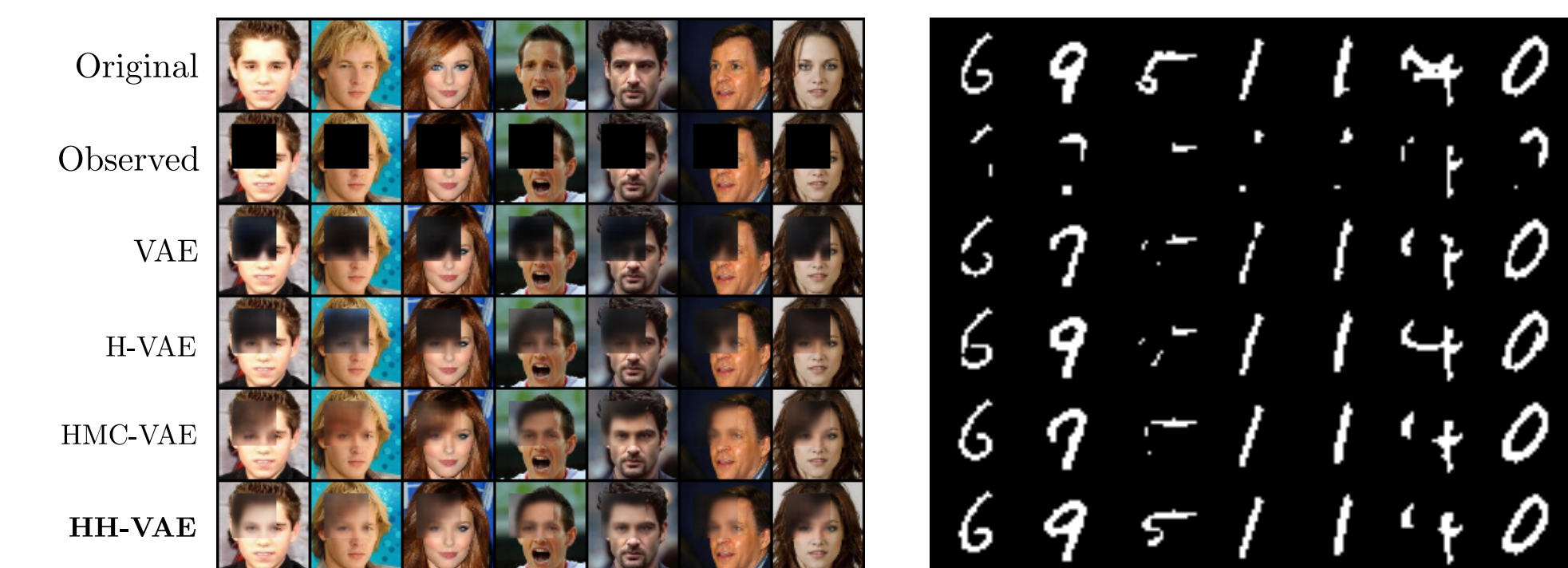


Figure 5: Image conditional inpainting on CelebA (left) and MNIST (right)

Acknowledgements

Ignacio Peis acknowledges support from Spanish government MICIU under grants FPU18/00516, RTI2018-099655-B-I00, EST21/00467 and PID2021-123182OB-I00 and from Comunidad de Madrid under grants Y2018/TCS-4705 PRACTICO-CM and the Multiannual Agreement with UC3M in the line of Excellence of University Professors (EPU3M27), and in the context of the V PRICIT (Regional Programme of Research and Technological Innovation). José Miguel Hernández-Lobato acknowledges support from Boltzbit.

